Transient Responses in Delaminated Composite Plates with Integrated Active Fiber Composite Patches as Actuators and Sensors

Ganesh Shankar[a], Ashes Maji[b] , P.K.Mahato[c]

[a]Associate Professor, Mechanical Engineering Department , Dumka Engineering College (Estd. by Govt. of Jharkhand and run by Techno India under PPP) Jharkhand 814101 India

[b]Assistant Professor Mechanical Engineering Department Asansol Engineering College Asansol, West Bengal

[c]Associate Professor Department of Mechanical Engineering, Indian Institute of Technology(Indian School of Mines), Dhanbad 826004, India

Abstract:

This study investigates the transient response of composite plates with centrally located delaminations. A finite element model is developed where the deformation along both the healthy and delaminated regions is formulated based on the First-Order Shear Deformation Theory (FSDT). The governing equations are derived using the minimum total potential energy principle. The model utilizes an eight-nodded serendipity element with five degrees of freedom per node and is implemented computationally in MATLAB. A key focus of the analysis is a parametric study examining the influence of boundary conditions and the size of small delaminations (6%, 8%, and 10% of the total plate area) on the dynamic displacement responses. The results conclusively demonstrate a significant amplification of transient vibrations due to the presence of Delaminations damage, quantifying its detrimental effect on the structural dynamic performance.

Keywords: Delaminations, Composite Plates, Transient Analysis, Finite Element Method (FEM), First-Order Shear Deformation Theory (FSDT), Structural Dynamics

Introduction

Composite materials are extensively used in aircraft industries, marine engineering, sports industries and automobile sectors in various applications due to its well known property such as light weight and high strength. Composite laminate usually go through the repeated cyclic stress and other external impact during service, which results delamination or debonding between plies of laminates. Delamination degrades the stiffness and strength of composite structures and simultaneously high deformation along longitudinal and transverse direction is occurred because of increased residual stress in between laminae. A smart structural model is required to compensate the undesirable response. An Active fiber composite (AFC) is kind of piezoelectric fiber which have high actuation and sensing capability in active structure. The key features of AFC over conventional piezoceramics actuators/sensors are high strength; directional actuation

and low insertion cost, Hence, AFC are used in controllable structures, to get required strength and/or stiffness, and to perform the required tasks.

Plenty of research articles are available on laminated composite plate modeling. They can be broadly classified into equivalent single layer (ESL) theories [1] and layerwise theory (LW) [2, 3]. ESL theories can further be classified into classical plate theory (CPT) [4], first order shear deformation theory (FSDT) [5], higher order shear deformation theory (HSDT) [6], and zigzag theory [7]. A detailed review on the type of plate theories available and their applicability is presented by Zhang and Yang [8] and R. Khandan et al. [9]. Delamination refers to a defect associated with the laminated structures. The cause of delamination may be either due to imperfect fabrication techniques (air entrapment or residual stresses), or due to fatigue loads during the service period of the structure. Due to delamination in composite structures, structural stiffness degrades. The study of delamination is mainly categorized into two approaches: (i) Region wise approach: In this approach laminate is divided into sublaminates i.e. healthy laminated region and delaminated region. The continuity condition is applied at the interface of healthy and delaminated sub-laminates [10], (ii) Layer wise model approach: This approach is based on layer wise theory in which layer-by-layer approximation of displacement fields in thickness direction is considered. At the delamination interface, the displacement continuity conditions are not enforced.

Several research works are available on dynamics analysis of delaminated composite plates such as, Campanelli and Engblom [11] studied dynamic behaviour of graphite/peek composite plate. Author [11] discussed the natural frequencies of graphite/peek plate under mid-plane and corner delamination. Saravanos and Hopkins [12] have formulated the generalised stiffness, inertia and damping matrices of delaminated composite beam for the purpose of calculate natural frequencies and mode shape beam. Free and forced vibration study of twisted-delaminated composite plates which are highly used in turbine blades and helicopter fans are elaborated by Parhi et al. [13]. Dynamic study of multiple delaminations in laminate is discussed by Jinho et al. [14], author applied the Lagrange multiplier method for time integration analysis to avoid the penetration problem in delaminated region.

In this study AFC patches are used as actuator and sensor to observe the transient vibratory responses. The Electro-mechanical formulation is based on first order shear deformation theory. The finite element analysis of AFC patches and delaminated plate is coded in MATLAB. The dynamic response is extracting by the help of Newmark’s time integration scheme. The transient vibratory responses have been obtained in different boundary conditions, and AFC patch location, in presence of small delamination on the laminated plate.

Mathematical formulation

The constitutive equations of Electro-Elastic relationship are given in Equation (1) and (2). Equation (1) corresponds to the in-plane stress-strain and shear stress-strain relationship and

Equation (2) corresponds to the electro-mechanical displacement due to AFC (active fiber composite) is given as following.

$$\begin{Bmatrix}\sigma_{11}\\ \sigma_{22}\\ \sigma_{12}\end{Bmatrix}=\begin{bmatrix}Q_{11} & Q_{12} & 0\\ Q_{21} & Q_{22} & 0\\ 0 & 0 & Q_{66}\end{bmatrix}\begin{Bmatrix}\varepsilon_{11}\\ \varepsilon_{22}\\ \varepsilon_{12}\end{Bmatrix}-\begin{bmatrix}e_{11} & 0 & 0\\ e_{12} & 0 & 0\\ 0 & 0 & 0\end{bmatrix}\begin{Bmatrix}E_1\\ E_2\\ E_3\end{Bmatrix} \quad (1)$$

$$\begin{Bmatrix}\sigma_{23}\\ \sigma_{13}\end{Bmatrix}=\begin{bmatrix}Q_{44} & 0\\ 0 & Q_{55}\end{bmatrix}\begin{Bmatrix}\varepsilon_{23}\\ \varepsilon_{13}\end{Bmatrix}-\begin{bmatrix}0 & e_{42} & 0\\ 0 & 0 & e_{53}\end{bmatrix}\begin{Bmatrix}E_1\\ E_2\\ E_3\end{Bmatrix}$$

$$\begin{Bmatrix}D_1\\ D_2\\ D_3\end{Bmatrix}=\begin{bmatrix}e_{11} & e_{12} & 0 & 0 & 0\\ 0 & 0 & 0 & e_{43} & 0\\ 0 & 0 & 0 & 0 & e_{53}\end{bmatrix}\begin{Bmatrix}\varepsilon_{11}\\ \varepsilon_{22}\\ \varepsilon_{12}\\ \varepsilon_{23}\\ \varepsilon_{13}\end{Bmatrix}+\begin{bmatrix}\kappa_{11} & 0 & 0\\ 0 & \kappa_{22} & 0\\ 0 & 0 & \kappa_{33}\end{bmatrix}\begin{Bmatrix}E_1\\ E_2\\ E_3\end{Bmatrix} \quad (2)$$

Where, $\{\sigma_{ij}\}$ is the stress vector $[Q_{ij}]$ is the constitutive matrix, $\{\varepsilon_{ij}\}$ is the strain vector due to mechanical loading, $\{D_i\}$ is the electric displacement, $[e_{ij}]$ is the piezoelectric stress coefficient matrix, $[\kappa]$ is the dielectric constant, $\{E_i\}$ is the electric field vector.

If V is the electric potential difference between the two electrodes and h_{et} is the distance between two electrodes and we assuming the electric field is acting along the X-direction so the electric field vector can be written as

$$\begin{Bmatrix}E_1\\ E_2\\ E_3\end{Bmatrix}=\begin{Bmatrix}-1/h_{et}\\ 0\\ 0\end{Bmatrix}V \quad (3)$$

In above equations (1-3), the constitutive relations are in material co-ordinate systems. Each lamina may have different orientations with respect to global or structural co-ordinate system; hence the co-ordinate transformation from the material co-ordinate system to the structural co-ordinate system is required. If the lamina is oriented at an angle θ with respect to the structural/global reference frame then the in-plane strain transformation matrix is given by

$$\begin{Bmatrix}\varepsilon_X\\ \varepsilon_Y\\ \varepsilon_{XY}\end{Bmatrix}=\begin{bmatrix}m^2 & n^2 & -2mn\\ n^2 & m^2 & 2mn\\ mn & -mn & m^2-n^2\end{bmatrix}\begin{Bmatrix}\varepsilon_{11}\\ \varepsilon_{22}\\ \varepsilon_{12}\end{Bmatrix} \quad (4)$$

Similarly shear strain transformation matrix is given by;

$$\begin{Bmatrix} \varepsilon_{YZ} \\ \varepsilon_{XZ} \end{Bmatrix} = \begin{bmatrix} m & -n \\ n & m \end{bmatrix} \begin{Bmatrix} \varepsilon_{23} \\ \varepsilon_{13} \end{Bmatrix} \tag{5}$$

Where $m=\cos\theta$ and $n=\sin\theta$

If the piezoelectric layers are oriented at angle θ_p with X-axis then piezoelectric stress coefficient matrix $[e]$ is transformed into $[e]_{xy}$ and can be written as

$$[e]_{xy} = \begin{bmatrix} m^2 & n^2 & 2mn \\ n^2 & m^2 & -mn \\ -mn & mn & m^2 - n^2 \end{bmatrix} [e] \begin{bmatrix} m & -n & 0 \\ -n & m & 0 \\ 0 & 0 & 0 \end{bmatrix} \tag{6}$$

Where $m=\cos\theta_{p\ and}$ $n=\sin\theta_p$.

Finite element formulation and stress resultant matrix for healthy plate element

Element for a healthy plate based on the first order displacement theory is applied. An eight nodded serendipity element, with five degrees of freedom at each node is adopted here for element formulation. Displacement fields are interpolated using Lagrangian shape function as follows.

$$u_0 = \sum_{i=1}^{8} N_i u_i \quad , \; v_0 = \sum_{i=1}^{8} N_i v_i \quad , w_0 = \sum_{i=1}^{8} N_i w_i \quad , \theta_x = \sum_{i=1}^{8} N_i \theta_{x_i} \quad , \theta_y = \sum_{i=1}^{8} N_i \theta_{y_i} \tag{7}$$

Where u_i, v_i, w_i are the nodal displacements θ_{xi}, θ_{yi} are nodal rotation degree of freedom along mid-plane and N_i is the shape function of corresponding node. Now strain-displacement relation is deriving from above equation.

$$\{\varepsilon\} = [\partial] \sum N_i \{\delta\} = \sum [\partial N_i] \{\delta\} \quad \text{Or} \quad \{\varepsilon\} = \sum [B_i] \{\delta\} \tag{8}$$

The stress-resultants can be obtained by integrating the stresses through the thickness of the laminate. The stress resultants due to mechanical loading is given by

$$\begin{Bmatrix} N_x \\ N_y \\ N_{xy} \\ M_x \\ M_y \\ M_{xy} \end{Bmatrix} = \begin{bmatrix} A & B \\ B & D \end{bmatrix} \begin{Bmatrix} \varepsilon_x \\ \varepsilon_y \\ \gamma_{xy} \\ k_x \\ k_y \\ k_{xy} \end{Bmatrix}$$

$$[A_{ij}] = \sum_{k=1}^{N} \left[Q_{ij} \right]_k (z_k - z_{k-1})$$

$$[B_{ij}] = \frac{1}{2} \sum_{k=1}^{N} \left[Q_{ij} \right]_k (z^2{}_k - z^2{}_{k-1})$$

$$[D_{ij}] = \frac{1}{3} \sum_{k=1}^{N} \left[Q_{ij} \right]_k (z^3{}_k - z^3{}_{k-1}) \tag{9}$$

Here N_x, N_y, and M_x, M_y, are the normal forces and bending moment along X, Y axis where and N_{xy} and M_{xy} are in-plane shear force and twisting moment. $[A_{ij}]$=extensional stiffness matrix, $[B_{ij}]$ = extension-bending coupling matrix, $[D_{ij}]$ =bending stiffness matrix, $[Q_{ij}]_k$=constitutive stiffness matrix of lamina

Shear stress and strain relation in matrix form is as follows

$$\begin{Bmatrix} Q_x \\ Q_y \end{Bmatrix} = k_{scf} \left[G_{ij} \right] \begin{Bmatrix} \gamma_{xz} \\ \gamma_{yz} \end{Bmatrix} \tag{10}$$

$$\left[G_{ij} \right] = \sum_{k=1}^{N} \begin{bmatrix} Q_{55} & Q_{45} \\ Q_{45} & Q_{44} \end{bmatrix} (Z_k - Z_{k-1})$$

Where Q_x and Q_y are the shear forces per unit length along XZ and YZ plane respectively. k_{scf}=shear correction factor (k_{scf}=5/6) and z = coordinate along depth and Z_k-Z_{k-1}=thickness of each lamina and Q_{44} , Q_{45} , Q_{55} modulus of rigidity .

Finite element procedure for Delamination modelling

Laminated plate is divided into sub-laminate i.e. delaminated and healthy regions and analyzed separately. In Fig. 1, ‘abcd’ is delaminated area of laminated plate, so the laminate is also split into upper delaminated sub-laminate and lower delaminated sub-laminate.

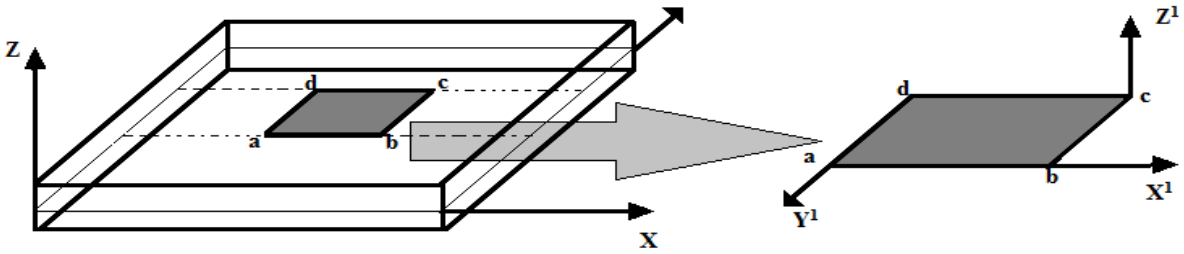

Fig. 1. Isometric view and coordinate system of delaminated plate

If a single delamination is present at the middle of the plate, then the upper and lower segment of the delaminated region is meshed separately. The coordinate system of delaminated segment is x^1, y^1, z^1. The z co-ordinate remains the same for the integral laminate as well as the delaminated sub-laminates, this way, we account for the eccentricities of the sub-laminate mid-planes with respect to the mid-plane of the integral laminate. So, according to the first order shear deformation theory, displacement field variable in the delaminated region is given below, similarly, for the sub-laminate displacement field for sub-laminate is obtained by changing the subscript.

$$u_B(x^1, y^1) = u_B^0 + z\theta_{x_B}$$
$$v_B(x^1, y^1) = v_B^0 + z\theta_{y_B} \quad (11)$$
$$w_B(x^1, y^1) = w_B^0$$

If ‘p’ is the number of layers in the lower delaminated part and N is the total number of layers then the bending stiffness matrix and density matrix is changed according to Equation (12)

Lower delamination bending stiffness

$$[A_{ij}]_L = \sum_{k=1}^{p} [Q_{ij}]_k (Z_k - Z_{k-1})$$
$$[B_{ij}]_L = \frac{1}{2} \sum_{k=1}^{p} [Q_{ij}]_k (Z^2{}_k - Z^2{}_{k-1})$$
$$[D_{ij}]_L = \frac{1}{3} \sum_{k=1}^{p} [Q_{ij}]_k (Z^3{}_k - Z^3{}_{k-1})$$

Upper delamination bending stiffness

$$[A_{ij}]_U = \sum_{k=p+1}^{N} [Q_{ij}]_k (Z_k - Z_{k-1})$$
$$[B_{ij}]_U = \frac{1}{2} \sum_{k=p+1}^{N} [Q_{ij}]_k (Z^2{}_k - Z^2{}_{k-1}) \quad (12)$$
$$[D_{ij}]_U = \frac{1}{3} \sum_{k=p+1}^{N} [Q_{ij}]_k (Z^3{}_k - Z^3{}_{k-1})$$

$$\begin{bmatrix} D_L \end{bmatrix} = \begin{bmatrix} a & b \\ b & d \end{bmatrix}_L \text{ And } \begin{bmatrix} D_U \end{bmatrix} = \begin{bmatrix} a & b \\ b & d \end{bmatrix}_U$$

From the above *A,B,D* matrices we have to calculate the D_L and D_U matrices for lower and upper delaminated segment element and then calculate the stiffness and mass matrix of delaminated element. The stiffness and mass matrices calculations for the upper and lower sub-laminates will follow similar procedure as mentioned earlier for the healthy laminate.

Boundary condition:

Three types of boundary condition are considered here for the numerical simulation in present article, which are S-S-S-S, C-F-F-F and C-C-C-C. Here ‘S’ stands for the simply supported edge, ‘C’ stand for clamped edge and ‘F’ for free edge. The prescribed displacements and rotations for the above mentioned boundary conditions are:

S-S-S-S boundary condition (Simply-supported)

at $Y = 0,\ Y = b$

$u = 0,\ v \neq 0,\ w = 0,\ \theta_x = 0,\ \theta_y \neq 0$

C-F-F-F condition (Cantilever)

at $X = 0$

$u = 0,\ v = 0,\ w = 0,\ \theta_x = 0,\ \theta_y = 0$

In C-C-C-C boundary condition.

at $X = 0$ and $X = a$ at $Y = 0$ and $Y = b$

$u = 0,\ v = 0,\ w = 0,\ \theta_x = 0,\ \theta_y = 0$ $u = 0,\ v = 0,\ w = 0,\ \theta_x = 0,\ \theta_y = 0$

Here a= length of the plate along X-axis and b= breath of the plate along Y-axis

3. Results and Discussion

A finite element model developed in MATLAB is used to generate the numerical results presented in this section. The model features Active Fiber Composite (AFC) patches attached to the upper and lower surfaces of the plate. The electro-mechanical behavior of these patches is directly simulated within the finite element code. The parametric investigation focuses on the impact of AFC patch placement, varying sizes of initial mid-plane delaminations, and different boundary conditions. Corresponding material properties for the graphite/epoxy composite and the AFC material are detailed in Table 1.

Table 1. Material properties of graphite/epoxy and AFC -50% fiber volume fraction.

Elastic module	graphite/epoxy [16]	AFC layer [16]
E_{11} (Gpa)	128	119.7
E_{22} (Gpa)	6.12	129.1
μ_{12}	0.3	0.35
μ_{13}	---	0.38
G_{12} (Gpa)	5.0	39.14
G_{13} (Gpa)	5.0	32.35
G_{23} (Gpa)	2.5	32.35
$e_{11}(c/m^2)$	---	14.14
$e_{21}(c/m^2)$	---	-3.34
$e_{24}(c/m^2)$	---	10.79
$\kappa_{11}(F/m)$	---	8.599×10^{-9}
$\kappa_{33}(F/m)$	---	6.485×10^{-9}
Density (Kg/m^3)	1600	6700

At first an example is presented to validate the current approach. A rectangular cantilever plate of ply orientation $[0/90]_{4s}$ and geometry $0.311m\times0.051m\times0.00218m$ is considered. A PZT sensor is bounded at a distance of $0.0207m$ from fixed end. The size of the piezoelectric sensor is $0.0415m\times0.0255m\times0.00025m$. A delamination of size $0.104m\times0.051m$ is considered at a distance of $0.104m$ from the fixed end and located at the second interface from the mid-surface. A constant load $10N$ is acting on free end of plate. The material properties of PZT sensor and composite laminae are given in Ref. (Ghoshal et al. 2005)[15] The linear deflection of smart healthy and delaminated plate in time history is obtained from current approach, and compared with the data available in article (Ghoshal et al. 2005) in which layer wise approach is used; a good correlation is obtained while comparing the results is shown in Fig.2 (healthy plate) and Fig 3 (delaminated plate).

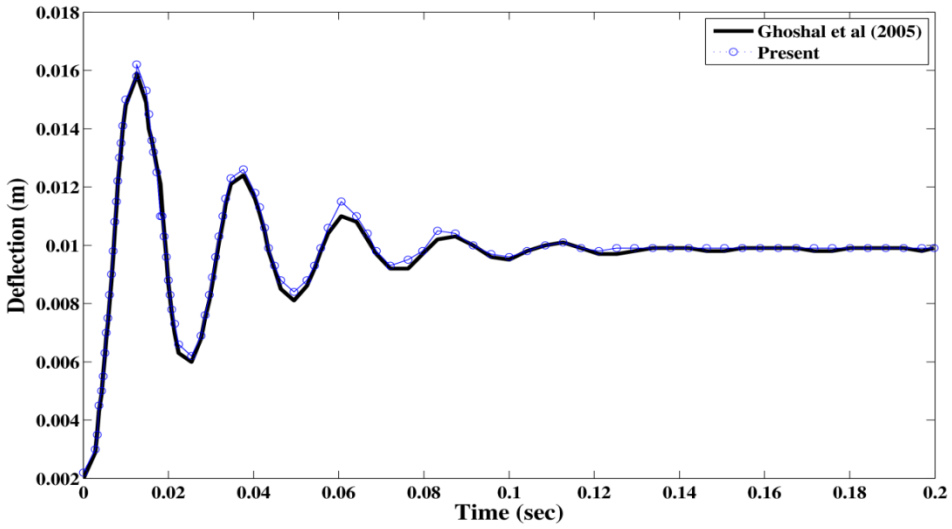

Fig.2 Linear transient response of healthy plate.

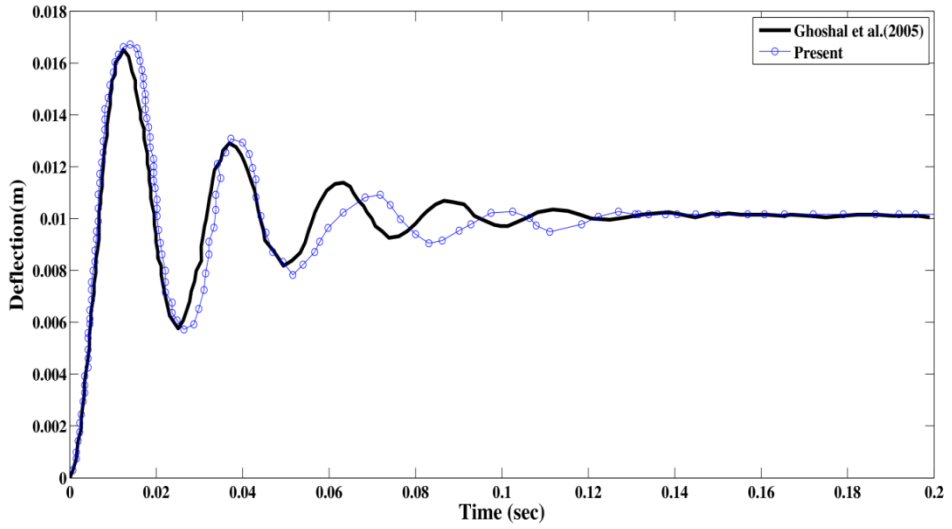

Fig.3 Linear transient response of delaminated plate.

Model Description and Loading: The subject of this study is an asymmetric laminated square plate (0.6 m × 0.6 m × 0.006 m) with a stacking sequence of (90/0/90/0). A square delamination of varying sizes—6%, 7%, 8%, 9%, and 10% of the total plate area—is located at the midplane shown in Fig 4.

Numerical Setup: The plate is discretized using an 8×8 mesh. The space between two electrodes is specified as 0.00025 m.

Boundary and Loading Conditions: The analysis encompasses three boundary conditions:

- Simply supported on all edges (S-S-S-S).
- Cantilevered (C-F-F-F), with one edge clamped and the others free.
- Fully clamped (C-C-C-C).

A point load of 1000 N is applied at the geometric center for the S-S-S-S and C-C-C-C cases. For the cantilevered case (C-F-F-F), the load is applied at the midpoint of the free edge.

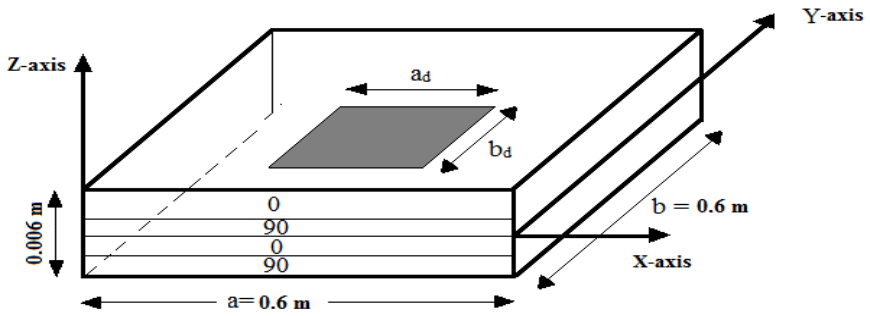

Fig. 4 Plate geometry and delamination location

Figure 5 shows the AFC patches position at different location on both side of plate. Here, two different location of patches position is discussed for the dynamics analysis of delaminated composite plate. Dimension of AFC patches which is shown in Figure 5 (a), 5 (b), are discussed in Table 2. Figure 5(a) shows the AFC patch position 1 which is away from the delaminated region and Figure 5(b) shows the AFC patch position 2 which is likely same dimension as the size of delamination details are given in Table 2.

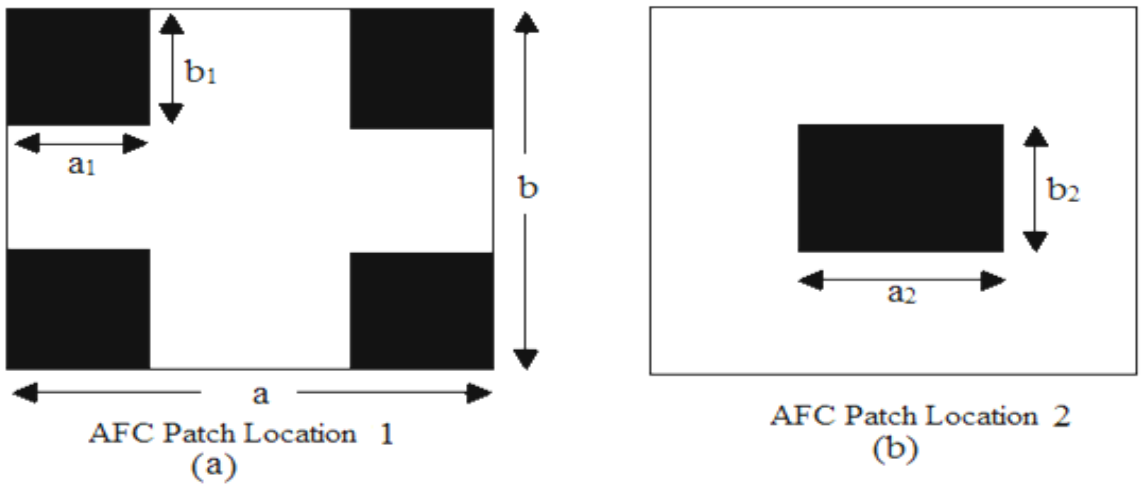

Fig. 5 AFC patches location at different places on plate

Table 2. Dimensions of delaminated region and AFC patches.

Delamination along midplane (% of total area)	Size of delamination $a_d \times b_d$ (m) **Refer figure 2**	AFC patch location 1 $a_1 \times b_1$ (m) **Refer figure 3(a)**	AFC patch location 2 $a_2 \times b_2$ (m) **Refer figure 3(b)**
6% delamination	0.14697×0.14697	0.2265× 0.2265	0.14697×0.14697
7% delamination	0.15874 ×0.15874	0.2206×0.2206	0.15874 ×0.15874
8% delamination	0.16970 ×0.16970	0.2151×0.2151	0.16970 ×0.16970
9% delamination	0.18×0.18	0.21 ×0.21	0.18×0.18
10% delamination	0.18974×0.18974	0.2051×0.2051	0.18974×0.18974

Transient analysis of delaminated and without delaminated plate in various boundary conditions.

Transient analysis of delaminated and without delaminated plate is studied in this section. A point load of 1000*N* is applied at middle of the plate in simply supported (S-S-S-S) and clamped-clamped boundary (C-C-C-C), whereas it will be act at midpoint of free end in C-F-F-F boundary condition.

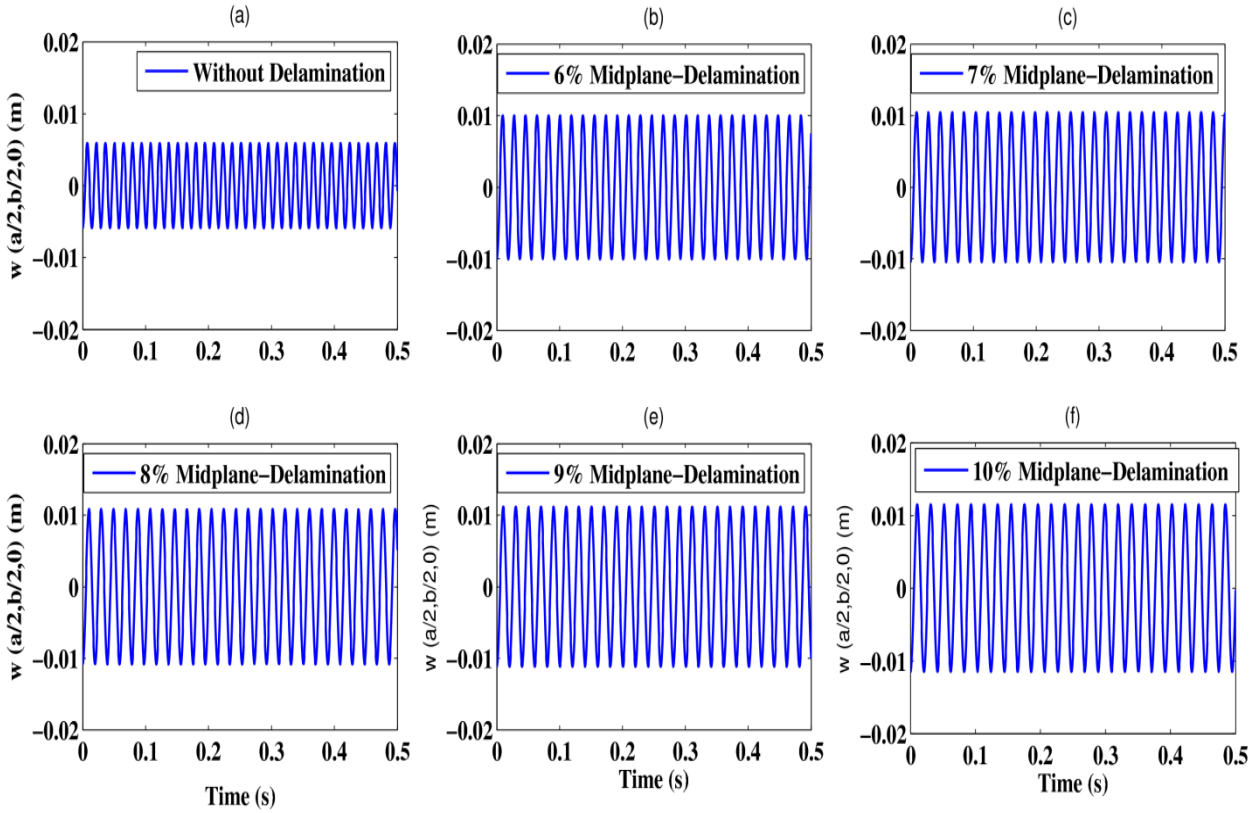

Fig. 6 Time response of delaminated and without delaminated plate in S-S-S-S boundary condition.

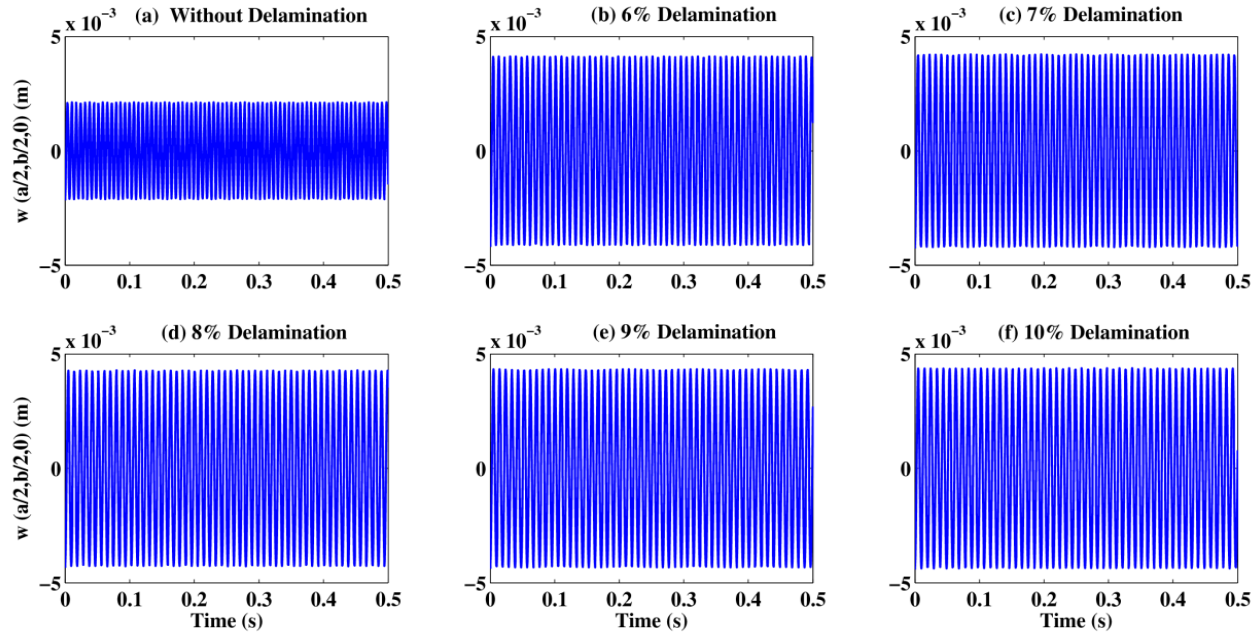

Fig. 7 Time response of delaminated and without delaminated plate in C-C-C-C boundary condition.

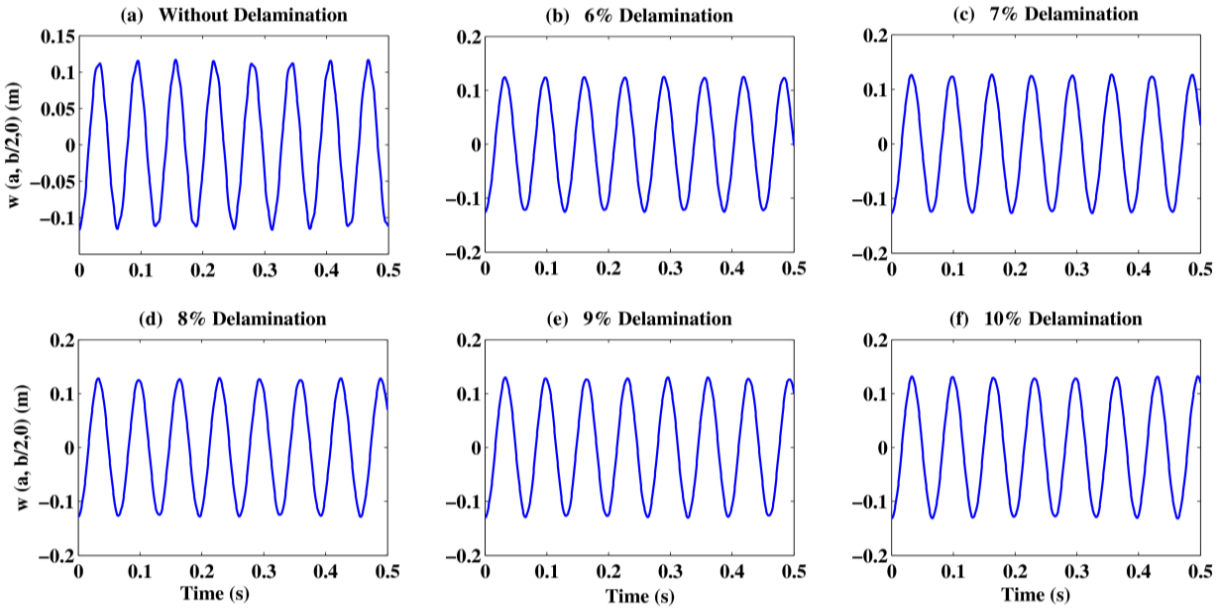

Fig. 8 Time response of delaminated and without delaminated plate in C-F-F-F boundary condition.

Figure 6 shows the dynamic response in time history under S-S-S-S boundary condition with and without delamination; here various delamination sizes i.e 6%,7%, 8%, 9%, 10% and without delamination are taken into consideration. Similarly Figure 7 and Figure 8 have discussed same relationship in C-C-C-C and C-F-F-F boundary conditions. It is clear from Figure 6, Figure 7,

and Figure 8 that as the delamination introduce in the structure the dynamic displacement amplitude is increased and it is steady state response.

Table 3. Maximum amplitude (meter) in various delamination sizes under different boundary condition

	S-S-S-S	C-C-C-C	C-F-F-F
No delamination	0.0059	0.0021176	0.11671969
6% delamination	0.0100	0.0041349	0.12496376
7% delamination	0.0104	0.0042132	0.12707631
8% delamination	0.0108	0.0042763	0.12863563
9% delamination	0.0112	0.0043272	0.13001410
10% delamination	0.0116	0.0044695	0.13174240

Table 3 shows the maximum amplitude of plate structure in different delamination sizes under various boundary conditions. It is seen from tabulate results that the maximum amplitude is increases as the size of delamination increases. In S-S-S-S boundary condition the maximum peak of amplitude under no delamination is 0.0059*m* while it is increased by 69.5%, 76.3%, 83%, 89.8% and 96.6% under 6%, 7%, 8%, 9% and 10% delamination. Similarly in C-C-C-C and C-F-F-F boundary condition the maximum amplitude under no delamination is noted 0.00211*m* and 0.117*m* respectively. In C-F-F-F boundary condition (refer figure 8) the dynamic displacement response is not much affected under delamination.

Conclusion

This study successfully investigates the transient dynamic responses of delaminated composite plates integrated with Active Fiber Composite (AFC) patches acting as actuators and sensors. A finite element model based on the First-Order Shear Deformation Theory (FSDT) was developed in MATLAB to simulate the electro-mechanical behavior of the smart composite structure. The model effectively captures the effects of delamination size, AFC patch placement, and various boundary conditions on the dynamic response of the plate.

Key findings include:

- The presence of delamination significantly increases the amplitude of transient vibrations, with larger delamination sizes leading to greater dynamic displacements.
- The effect of delamination is most pronounced in simply-supported (S-S-S-S) and fully clamped (C-C-C-C) boundary conditions, where amplitude increases of up to **96.6%** were observed for a 10% delamination area.
- In cantilevered (C-F-F-F) boundary conditions, the influence of delamination on dynamic response was less severe, though still noticeable.
- The placement of AFC patches (both near and away from the delamination) was shown to be feasible for sensing and actuation purposes, supporting their use in health monitoring and vibration control of composite structures.

The developed model was validated against existing literature, showing good agreement for both healthy and delaminated plates. This work contributes to the understanding of damage detection and dynamic behavior in smart composite structures and provides a foundation for future research into real-time monitoring and adaptive control of delaminated composites.

References

[1]. R. Kienzler, On consistent plate theories, Archive of Appl. Mech. 72(2002) 229-247.

[2]. J. N. Reddy, An evaluation of equivalent-single-layer and layerwise theories of composite laminates, Compos. Struct. 25 (1993) 21-35.

[3]. M. Marjanović, D. Vuksanović, Layerwise solution of free vibrations and buckling of laminated composite and sandwich plates with embedded delaminations, Compos. Struct. 108 (2014) 9-20.

[4]. J.N. Reddy, Mechanics of laminated composite plates and shell, CRC Press, New York 2004.

[5]. R.P Shimpi, H.G. Patel, H. Arya, New first-order shear deformation plate theories, J. Appl. Mech. 74 (2007) 523-533.

[6]. G. Shi, A new simple third-order shear deformation theory of plates, Int. J. solids and struct. 44 (2007) 4399-4417.

[7]. S. Kapuria, G.G.S. Achary, An efficient higher order zigzag theory for laminated plates subjected to thermal loading, Int. J. Solids and Struct. 41 (2004) 4661-4684.

[8]. Y. X. Zhang, C. H. Yang, Recent developments in finite element analysis for laminated composite plates, Compos. Struct. 88 (2009) 147-157.

[9]. R. Khandan, S. Noroozi, P. Sewell, J. Vinney, The development of laminated composite plate theories: a review, J. Materials Sci. 47 (2012) 5901-5910.

[10]. C.N. Della, D. Shu, Vibration of delaminated composite laminates: A review, Appl. Mech. Revie. 60 (2007) 1-20.

[11]. R.W.Campanelli, J.J. Engblom, The effect of aminations in graphite/PEEK composite plates on modal dynamic characteristics, Compos. struct. 31 (1995) 195-202.

[12]. Saravanos, Dimitris A., and D. A. Hopkins. "Effects of Delaminations on the Damped Dynamic Characteristics of Composite Laminates: Analysis and Experiments." Journal of Sound and Vibration (1996) **192**(5), 977–993.

[13]. Parhi PK, Bhattacharyya SK, Sinha PK. Dynamic analysis of multiple delaminated composite twisted plates. Aircraft Engineering and Aerospace Technology. 1999 Oct 1;71(5):451-61.

[14]. Oh J, Cho M, Kim JS. Dynamic analysis of composite plate with multiple delaminations based on higher-order zigzag theory. International Journal of Solids and Structures. 2005 Nov 30;42(23):6122-40.

[15]. Ghoshal A, Kim HS, Kim J, Choi SB, Prosser WH, Tai H. Modeling delamination in composite structures by incorporating the Fermi–Dirac distribution function and hybrid damage indicators. Finite elements in analysis and design. 2006 May 31;42(8):715-25.

[16]. P.K.Mahato, D.K. Maiti, Aeroelastic analysis of smart composite structures in hygro-thermal environment, Compos. Struct. 92 (2010) 1027-1038.